

# GNL3L inhibits activity of estrogen-related receptor $\gamma$ by competing for coactivator binding

Hiroaki Yasumoto, Lingjun Meng\*, Tao Lin\*, Qubo Zhu and Robert Y. L. Tsai<sup>‡</sup>

Center for Cancer and Stem Cell Biology, Alkek Institute of Biosciences and Technology, Texas A&M Health Science Center, Houston, TX 77030, USA

\*These authors contributed equally to this work

<sup>‡</sup>Author for correspondence (e-mail: rtsai@ibt.tamhsc.edu)

Accepted 22 May 2006

Journal of Cell Science 120, 2532-2543 Published by The Company of Biologists 2007

doi:10.1242/jcs.009878

## Summary

Guanine nucleotide binding protein-like 3 (GNL3L) is the closest homologue of a stem cell-enriched factor nucleostemin in vertebrates. They share the same yeast orthologue, *Grn1p*, but only GNL3L can rescue the growth-deficient phenotype in *Grn1*-null yeasts. To determine the unique function of GNL3L, we identified estrogen-related receptor  $\gamma$  (ERR $\gamma$ ) as a GNL3L-specific binding protein. GNL3L and ERR $\gamma$  are coexpressed in the eye, kidney and muscle, and co-reside in the nucleoplasm. The interaction between GNL3L and ERR $\gamma$  requires the intermediate domain of GNL3L and the AF2-domain of ERR $\gamma$ . Gain-of- and loss-of-function experiments show that GNL3L can inhibit the transcriptional activities of ERR genes in a cell-based reporter system, which does not require the

nucleolar localization of GNL3L. We further demonstrate that GNL3L is able to reduce the steroid receptor coactivator (SRC) binding and the SRC-mediated transcriptional coactivation of ERR $\gamma$ . This work reveals a novel mechanism that negatively regulates the transcriptional function of ERR $\gamma$  by GNL3L through coactivator competition.

Supplementary material available online at  
<http://jcs.biologists.org/cgi/content/full/120/15/2532/DC1>

Key words: ERR, Estrogen receptor, GNL3L, Nucleolus, Nucleostemin, SRC

## Introduction

Nucleostemin and its homologues, guanine nucleotide binding protein-like 3 (GNL3L) and *Ngp-1* (hereafter referred to as *Ngp1*), constitute a subfamily of GTP-binding proteins featured by their nucleolar distribution and a unique domain of circularly permuted GTP-binding motifs, where the G4 motif is located N-terminally to the G1, G2, and G3 motifs (Daigle et al., 2002; Leipe et al., 2002). Nucleostemin is enriched in the embryonic, mesenchymal and neural stem cells, in adult testes and several types of human cancers (Baddoo et al., 2003; Kafienah et al., 2006; Tsai and McKay, 2002). It plays a role in maintaining the continuous proliferation of neural stem cells (Tsai and McKay, 2002) and in regulating the protein stability of telomeric-repeat binding factor 1 (TRF1) (Zhu et al., 2006). Targeted deletion of nucleostemin leads to early embryonic lethality in homozygous nucleostemin-null embryos (Beekman et al., 2006; Zhu et al., 2006) and to premature senescence of heterozygous nucleostemin-null mouse embryonic fibroblast cells (Zhu et al., 2006).

Phylogenetically, nucleostemin is most closely related to GNL3L in vertebrates. They share the same yeast orthologue: *Grn1p* in *Schizosaccharomyces pombe* and *Nug1p* in *Saccharomyces cerevisiae*. *Grn1p* is involved in the processing of 35S pre-ribosomal RNA (rRNA), the nuclear export of Rpl25, and the maintenance of cell growth (Du et al., 2006). Mutation of *Nug1* inhibits the export of 60S subunit from the nucleolus (Du et al., 2006; Kallstrom et al., 2003). Although the yeast orthologue of nucleostemin and GNL3L displays

general activities in growth and ribosome biogenesis, rodent nucleostemin and GNL3L are distinctively expressed in different tissues. Furthermore, only human GNL3L, but not nucleostemin, can rescue the *Grn1*-deficient growth phenotype in fission yeasts (Du et al., 2006). These results suggest that nucleostemin and GNL3L have evolved specific properties in vertebrates, and become functionally diverged from each other and from *Grn1p*. By comparison, GNL3L retains more characteristics of *Grn1p* than does nucleostemin.

GNL3L bears 28% identity and 39% similarity to nucleostemin in mice. Very little is known about its function in vertebrates. To delineate the distinct activity of GNL3L, we looked for proteins that interact with GNL3L but not with nucleostemin. We first identified estrogen-related receptor  $\gamma$  (ERR $\gamma$ ) as a GNL3L-binding protein by a yeast two-hybrid screen, and confirmed this interaction by affinity-binding and coimmunoprecipitation assays. ERR $\gamma$  belongs to a subfamily of the nuclear receptor superfamily. The ERR gene family consists of three members, ERR $\alpha$ , ERR $\beta$ , and ERR $\gamma$ , that most resemble estrogen receptor  $\alpha$  (ER $\alpha$ ). Like ER $\alpha$ , the ERR proteins contain functionally separable structures that include an AF1 domain (or A/B region), a DNA-binding domain (DBD, or C region) with two zinc fingers, a hinge region (D), and a ligand-binding domain (LBD, or E/F region) with an AF2 domain at the C-terminal end. The LBD is involved in ligand binding, receptor dimerization, and coactivator binding. The AF2 domain is required for the ligand-dependent activation function. ERR $\alpha$  and ERR $\gamma$  are found in the brain, muscle,

heart, kidney and adipose tissues (Bonnelye et al., 1997; Giguere et al., 1988; Hong et al., 1999).  $ERR\beta$  is expressed in the eye, heart, kidney, cerebellum and testis (Bookout et al., 2006). The functions of the ERR family genes are implicated in many aspects of embryogenesis and tumorigenesis. Mice deficient in  $ERR\alpha$  exhibit reduced body weight and peripheral fat deposit, and are resistant to obesity induced by a high-fat diet (Luo et al., 2003).  $ERR\beta$ -null mice display placental defects, consistent with its role in the proliferation and differentiation of trophoblastic cells (Luo et al., 1997). In humans, the expression level of  $ERR\alpha$  correlates with poor prognosis in ovarian and breast cancers (Ariazi and Jordan, 2006; Suzuki et al., 2004). Conversely,  $ERR\gamma$  is a favorable indicator for human ovarian tumors (Sun et al., 2005). Although the ERR family genes are capable of binding the estrogen response element (ERE), they are different from  $ER\alpha$  in that their transcriptional activity and coactivator binding do not require ligand binding (Giguere et al., 1988; Hong et al., 1999; Kallen et al., 2004), which leaves open the question of whether the activities of the ERR family genes are constitutively active or dynamically regulated.

Here, we uncover a GNL3L-mediated pathway that regulates the transcriptional activity of the ERR family genes. We show that only GNL3L, but not nucleostemin or Ngp1, can interact with ERR family genes. Coexpression of GNL3L inhibits the transcriptional activities of the ERR family genes. Conversely, knocking down the endogenous expression of GNL3L increases the ERR-mediated transactivation. Furthermore, GNL3L can compete with steroid receptor coactivators (SRCs) for their  $ERR\gamma$  binding and block the SRC-mediated coactivation of  $ERR\gamma$ . Our study reveals a GNL3L-mediated mechanism that modulates the transcriptional activities of ERR proteins.

## Results

### GNL3L interacts with ERR family genes

To determine the unique function of GNL3L in vertebrates, we searched for proteins that interact with GNL3L but not with nucleostemin. A yeast two-hybrid approach was employed, where full-length GNL3L was fused to a GAL4 DNA binding-domain, and used to screen a mouse E17.5 brain cDNA library. From a total of 5 million clones screened, two positive clones were identified. They encoded the same in-frame partial sequence of  $ERR\gamma$  (Clone 43, residues 27-458). The interaction between GNL3L and clone 43 or full-length  $ERR\gamma$  was confirmed by affinity-binding assays in which agarose-bound GST fusion proteins of clone 43 and full-length  $ERR\gamma$ , but not the GST backbone protein, were able to retain hemagglutinin (HA)-tagged GNL3L specifically (Fig. S1A in supplementary material). We use coimmunoprecipitation assays to verify the interaction between GNL3L and  $ERR\gamma$  and to determine whether nucleostemin or Ngp1 can bind  $ERR\gamma$ . HEK293 cells were co-transfected with Myc-tagged  $ERR\gamma$  and one of the nucleostemin family genes tagged with an HA-epitope. Protein complexes were precipitated with anti-Myc or anti-HA antibodies, and immunodetected for the HA-tagged or Myc-tagged proteins (Fig. 1A). We found that only GNL3L, but not nucleostemin or Ngp1, was co-purified with  $ERR\gamma$  by anti-Myc immunoprecipitation (Fig. 1A, row 1). Consistently,  $ERR\gamma$  was detected only in the GNL3L protein complex, but not in the nucleostemin or Ngp1 protein complexes,

precipitated by anti-HA antibody (Fig. 1A, row 3). Like GNL3L,  $ERR\gamma$  belongs to a family of three genes. To determine whether GNL3L interacts with only  $ERR\gamma$  or with multiple members of the ERR gene family, HEK293 cells were transfected with HA-tagged GNL3L and Myc-tagged  $ERR\alpha$ ,  $ERR\beta$ , or  $ERR\gamma$  expression plasmids. Our results show that GNL3L and all members of the ERR gene family can be co-purified in the same protein complexes precipitated by either anti-Myc or anti-HA antibodies (Fig. 1B, rows 1 and 3). By contrast, no physical interaction between  $ERR\alpha$  (or  $ERR\beta$ ) and nucleostemin (or Ngp1) was detected by affinity-binding assays (Fig. S1B in supplementary material). Based on these results, we conclude that only GNL3L of the nucleostemin family can form stable protein complexes with the ERR family genes.

### $ERR\gamma$ colocalizes with GNL3L in the nucleoplasm

To determine whether the interaction between GNL3L and  $ERR\gamma$  is physiologically possible, we examined the expression patterns of GNL3L,  $ERR\beta$  and  $ERR\gamma$  by multi-tissue northern blot analyses. GNL3L was expressed most abundantly in the neural tissues, including the brain and eye, and was also detected in the muscle and kidney at low levels (Fig. 1C). Parallel blots showed that  $ERR\beta$  was expressed most abundantly in the kidney, followed by the eye, testis, heart and muscle. High-level expression of  $ERR\gamma$  was seen in the heart and eye, followed by the brain, kidney and muscle. To decide where within the cell this interaction might occur, green fluorescent protein (GFP)-tagged GNL3L or  $ERR\gamma$  were expressed in U2OS cells, which express both GNL3L and  $ERR\gamma$  endogenously. We found that GNL3L was distributed both in the nucleolus and in the nucleoplasm, whereas  $ERR\gamma$  was localized exclusively in the nucleoplasm (Fig. 1D). These data show that the tissue expression pattern of GNL3L correlates better with that of  $ERR\gamma$  than that of  $ERR\beta$ . Within the cell,  $ERR\gamma$  and GNL3L colocalize in the nucleoplasm. In the nucleolus, only GNL3L is found.

### The intermediate domain of GNL3L interacts with the AF2 domain of $ERR\gamma$

To gain insight into the functional importance of the GNL3L- $ERR\gamma$  interaction, we first identified the interacting domains of these two proteins using a panel of truncated GNL3L and  $ERR\gamma$  mutants (Fig. 2A,D). To define the  $ERR\gamma$ -binding domain in GNL3L, agarose-bound GST- $ERR\gamma$  fusion protein was used to pull down the wild-type and mutant GNL3L proteins (Fig. 2B). Our results show that  $ERR\gamma$  can bind GNL3L mutants that lack the BC-domain (dBC) or the G-domain (dG), as well as the N166I mutant that contains an Asn166 to Isl mutation in the G4 domain, which abolishes the GTP-binding capability of GNL3L (our unpublished data). Notably, the GST- $ERR\gamma$  fusion protein failed to retain mutants without the intermediate (I)-domain (dI and G31-G, Fig. 2B), indicating that the I-domain is necessary for the  $ERR\gamma$  binding of GNL3L. Different GNL3L mutants displayed distinctive subcellular distribution patterns not related to their  $ERR\gamma$ -binding abilities. The dBC and G31-G mutants were localized in the nucleoplasm and cytoplasm (Fig. 2C1,C2). The dG and dI mutants were localized more in the nucleolus than in the nucleoplasm (Fig. 2C3,C4), whereas the N166I mutant was diffusely distributed in the nucleus (Fig. 2C5). The  $ERR\gamma$

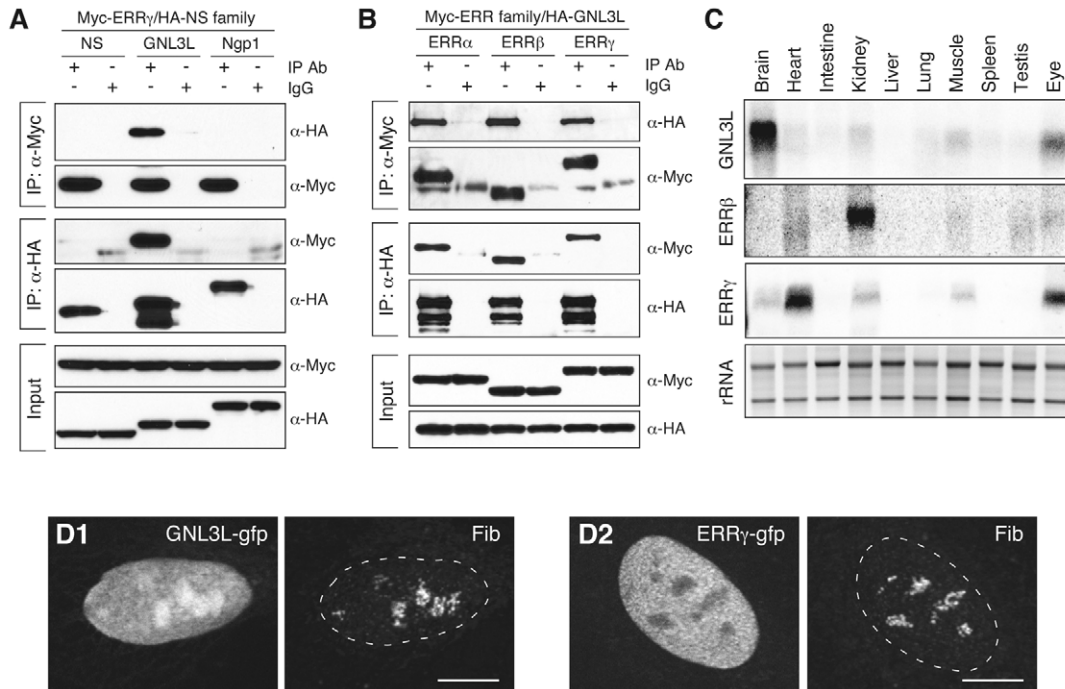


**Fig. 1.** GNL3L interacts with ERR $\alpha$ , ERR $\beta$  and ERR $\gamma$ . Protein interactions between ERR $\gamma$  and nucleostemin family genes (A) and between GNL3L and ERR family genes (B) were examined by *in vivo* coimmunoprecipitation assays. HEK293 cells were co-transfected with (A) Myc-tagged ERR $\gamma$  and HA-tagged nucleostemin, GNL3L or Ngp1 expression plasmids, or (B) HA-tagged GNL3L and Myc-tagged ERR $\alpha$ ,  $\beta$  or  $\gamma$  expression plasmids. Lysates were immunoprecipitated (IP) with anti-Myc antibody (rows 1 and 2,  $\alpha$ -Myc) or anti-HA antibody (rows 3 and 4,  $\alpha$ -HA). The co-purified proteins (rows 1 and 3) and the immunoprecipitates (rows 2 and 4) were immunodetected with the antibodies indicated on the right. Our results show that ERR $\gamma$  interacts only with GNL3L, not with nucleostemin or Ngp1, and that GNL3L binds all ERR family proteins. (C) Tissue distribution of GNL3L, ERR $\beta$  and ERR $\gamma$  in adult mice is shown by multi-tissue northern blots. GNL3L mRNA is expressed primarily in the neural tissues, including the brain and eye, and at lower levels in the kidney and muscle. The expression levels of GNL3L and ERR $\gamma$  match in kidney, muscle and eye, but differ in brain and heart. (D) In U2OS cells, the intensity of GFP-tagged GNL3L (GNL3L-gfp) is higher in the nucleolus than in the nucleoplasm. GFP-tagged ERR $\gamma$  (ERR $\gamma$ -gfp) is localized exclusively in the nucleoplasm. The nucleolar regions are labeled by anti-fibrillarin (Fib) antibody in the right panels. Dashed lines demarcate nucleo-cytoplasmic boundaries. Bars, 10  $\mu$ m.

protein structure consists of the AF1, DBD, LBD and AF2 domains (Fig. 2D). GST fusion proteins of the full-length ERR $\gamma$ , the AF1-domain deletion mutant (dAF1) and the LBD deletion mutant with an intact AF2-domain (dLBD) were able to bind wild-type GNL3L. By contrast, GST fusion proteins of the AF2-domain deletion mutant (dAF2), the last 245 residues containing the LBD and AF2 domains (LBD-AF2) and a mutant deleted of the LBD and AF2 domain (AF1-DBD) were unable to retain GNL3L, demonstrating that the AF2 domain is necessary but not sufficient for the binding of ERR $\gamma$  to GNL3L (Fig. 2E). Based on these results, we conclude that the interaction between GNL3L and ERR $\gamma$  requires the I-domain of GNL3L and the AF2 domain of ERR $\gamma$ , and is independent of the GTP binding and nucleolar localization of GNL3L.

#### Overexpression of a nucleolar form of GNL3L brings ERR $\beta$ and ERR $\gamma$ into the nucleolus

Given that GNL3L, but not ERR $\gamma$ , is localized in the nucleolus, we tested the idea whether coexpression of GNL3L can bring ERR $\gamma$  into the nucleolus. Using confocal analysis, we determined the distribution of ERR $\gamma$  when coexpressed with wild-type GNL3L (WT), a nucleolar form of GNL3L (NoG31), or an I-domain mutant of GNL3L fused to an SV40 nuclear localization sequence (NLS) (nls-I). NoG31 was created by

replacing the BC-domain of GNL3L with the BC-domain of nucleostemin (indicated by the grey bar in Fig. 3A) because nucleostemin has a stronger nucleolar localization capability than GNL3L and does not bind ERR $\gamma$ . The I-domain mutant was fused with an SV40 NLS because it lacks endogenous NLS of its own. Affinity-binding assays confirmed that both NoG31 and nls-I mutants were capable of binding ERR $\gamma$  (Fig. 3B). Whereas ERR $\gamma$  by itself was distributed outside of the nucleolus (Fig. 3C1,C1'), overexpression of wild-type GNL3L (Fig. 3C2,C2') and NoG31 (Fig. 3C3,C3') increased the ERR $\gamma$  fluorescence signal in the nucleolar region compared with cells expressing ERR $\gamma$  by itself. Notably, in cells overexpressing the NoG31 mutant, the ERR $\gamma$  signal accumulated in the nucleolar region, particularly in the periphery of the nucleolus. By contrast, the nls-I mutant failed to alter the ERR $\gamma$  distribution (Fig. 3C4), and distributions of wild-type GNL3L and NoG31 were unaltered by coexpression of ERR $\gamma$  (Fig. 3C2 vs C5, and C3 vs C6). Overexpression of GNL3L and its mutants exerts the same effects on the distribution of ERR $\beta$ . Whereas ERR $\beta$  by itself displayed a nucleoplasmic distribution (Fig. 3D1,D1'), both the wild-type GNL3L protein (Fig. 3D2,D2') and the NoG31 mutant (Fig. 3D3,D3') were able to increase the nucleolar intensity of ERR $\beta$ . By comparison, NoG31 had a stronger effect on bringing ERR $\beta$  into the nucleolus than wild-

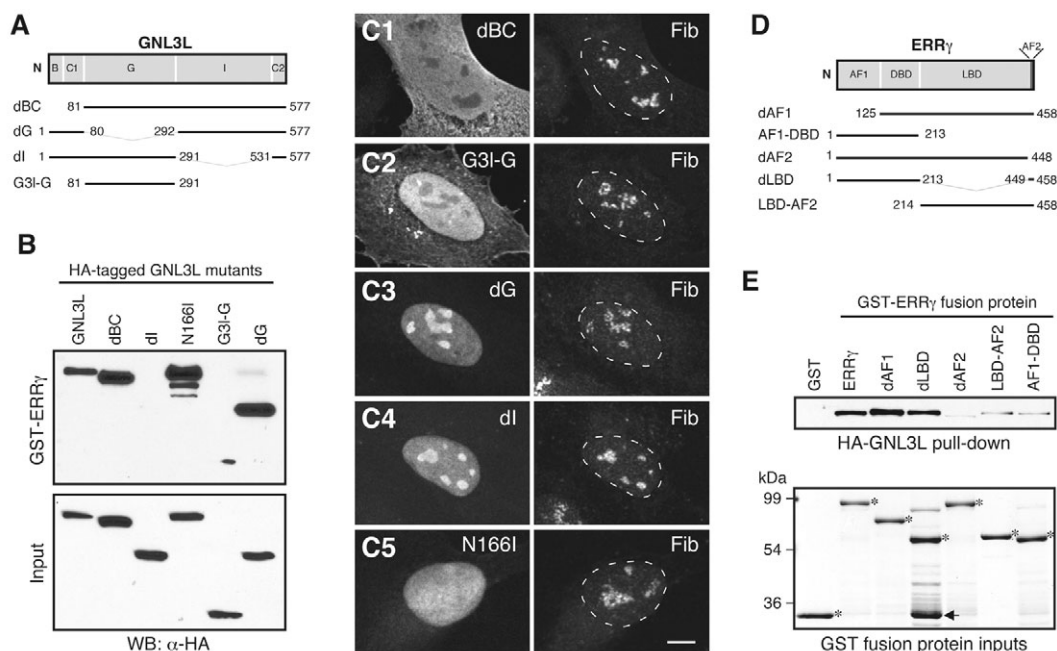


**Fig. 2.** Binding between GNL3L and ERR $\gamma$  requires the intermediate (I)-domain of GNL3L and the AF2-domain of ERR $\gamma$ . (A) Truncated mutants of GNL3L were used to determine its interacting domain with ERR $\gamma$ . B, basic domain; C1 and C2, coiled-coil domain-1 and -2; G, GTP-binding domain; I, intermediate domain. Numbers indicate amino acid positions. (B) GST-ERR $\gamma$  fusion proteins fail to bind mutants that lack the I-domain (dl and G3I-G) but can retain the dBC and the non-GTP-binding mutants, N166I and dG. (C) The subcellular distribution of HA-tagged dBC, G3I-G, dG, dl and N166I mutants are shown by confocal analyses double-labeled with anti-HA (left panels) and anti-fibrillarin (Fib, right panels) antibodies. Bar, 10  $\mu$ m. (D) Truncated mutants of ERR $\gamma$  were used to determine the domain interacting with GNL3L. AF1 and AF2, activation function 1 and 2; DBD, DNA-binding domain; LBD, ligand-binding domain. (E) Affinity-binding assays show that GST fusion proteins of the wild-type ERR $\gamma$ , the dAF1 mutant and the dLBD mutant can bind GNL3L, but GST fusion proteins of the dAF2, LBD-AF2 and AF1-DBD mutants cannot (top panel). The amount of GST fusion proteins used in each reaction, marked by asterisks, is shown in the bottom panel by Coomassie Blue staining. Some degradation occurs at the fusion site of the GST-dLBD protein (arrow).

type GNL3L. By contrast, overexpression of wild-type GNL3L or NoG3I had little or no effect on changing the distribution of ERR $\alpha$  (Fig. 3E). These results demonstrate that overexpression of a nucleolar form of GNL3L can change the distribution of ERR $\beta$  and ERR $\gamma$  in living cells, suggesting the possibility that nucleolar sequestration underlies the regulation of ERR $\beta$  and ERR $\gamma$  by GNL3L.

### GNL3L suppresses the transcriptional activities of ERR family genes

To investigate whether GNL3L can modulate the transcriptional activity of the ERR genes, an *in vivo* cell-based luciferase assay system was set up where CV-1 cells were co-transfected with a firefly luciferase reporter construct driven by three repeats of a consensus palindromic estrogen response element (ERE, see Materials and Methods), an ERR $\gamma$  expression plasmid, and a pRL-null reporter construct. The ERE-specific transcriptional activity was determined by the ratio between the Firefly and *Renilla* luciferase activities in the same sample, which represent ERE-driven and basal activities, respectively. This dual luciferase assay system was used to eliminate variations caused by transfection and non-specific effects on the common transcription-translational machinery. The Firefly-to-*Renilla* luciferase activity ratio for each experiment was expressed as the fold increase over the negative sample not transfected with ERR $\gamma$ . Our results show that ERR $\gamma$  can increase the ERE-specific transcriptional activity six

times higher than that of the control sample ( $6.0 \pm 0.5$ , mean  $\pm$  s.e.m.), and coexpression of GNL3L attenuates ERR $\gamma$ -dependent increase by 50% ( $2.9 \pm 0.2$ ) (Fig. 4A1, WT). This ERR $\gamma$  inhibitory effect of GNL3L requires its ERR $\gamma$ -interacting domain, because samples that coexpress the dl mutant fail to show such a repressive activity. To determine whether this inhibition is caused by nucleolar sequestration of ERR $\gamma$  by GNL3L, a nucleolar form of GNL3L (NoG3I) or a nucleoplasmic mutant of GNL3L (dBC) was coexpressed with ERR $\gamma$ . Our results demonstrate that both NoG3I and dBC can inhibit ERR $\gamma$ -mediated transcriptional activity more than or as much as the wild-type GNL3L. To test whether this transcriptional repressive effect of GNL3L can act on other members of the ERR family, we set up the same transactivational assay for ERR $\beta$  and ERR $\alpha$ . Our data show that GNL3L reduces the transcriptional activity of ERR $\beta$  from 4.7 times ( $\pm 0.3$ ) to 2.1 times ( $\pm 0.1$ ) over the control sample in an I-domain-dependent manner, and both NoG3I and dBC inhibit ERR $\beta$  as much as the wild-type protein (Fig. 4B1). Compared with ERR $\beta$  and ERR $\gamma$ , the ERR $\alpha$ -dependent increase of ERE-driven transactivation is less ( $2.7 \pm 0.1$ ). Although the wild-type GNL3L and the NoG3I mutant can reduce the ERR $\alpha$ -mediated transcriptional activity, the dBC mutant fails to do so (Fig. 4C1). The GNL3L effect on the transcriptional activities of the ERR family genes is specific, because GNL3L does not suppress estradiol (E2)-induced ERR $\alpha$ -mediated transactivation when using the same reporter

assay system ( $P=0.27$ , Fig. 4D). Finally, we confirm that these different effects of wild-type and mutant GNL3L on the transcriptional activities of ERR genes are not caused by different expression levels of the GNL3L or ERR proteins (Fig. 4A2,B2,C2).

To confirm the inhibitory effect of GNL3L from a loss-of-function angle, a small interfering RNA (siRNA) approach was used to knock down the expression of endogenous GNL3L in HEK293 cells. The knockdown efficiency of the GNL3L-

specific siRNA duplex-1 (siGNL3L-1) and duplex-2 (siGNL3L-2) was determined at the protein level in an HEK293 cell line that stably expresses HA-tagged GNL3L, and was estimated to be 83% and 84%, respectively, compared with the control siRNA knockdown sample (siNEG) (Fig. 5A). In siNEG-treated HEK293 cells, ERR $\gamma$  yielded an 11-fold induction on the ERE-driven transcription. In siGNL3L-1 and siGNL3L-2-treated cells, the ERR $\gamma$ -mediated transcriptional activities were significantly increased compared with the 11-

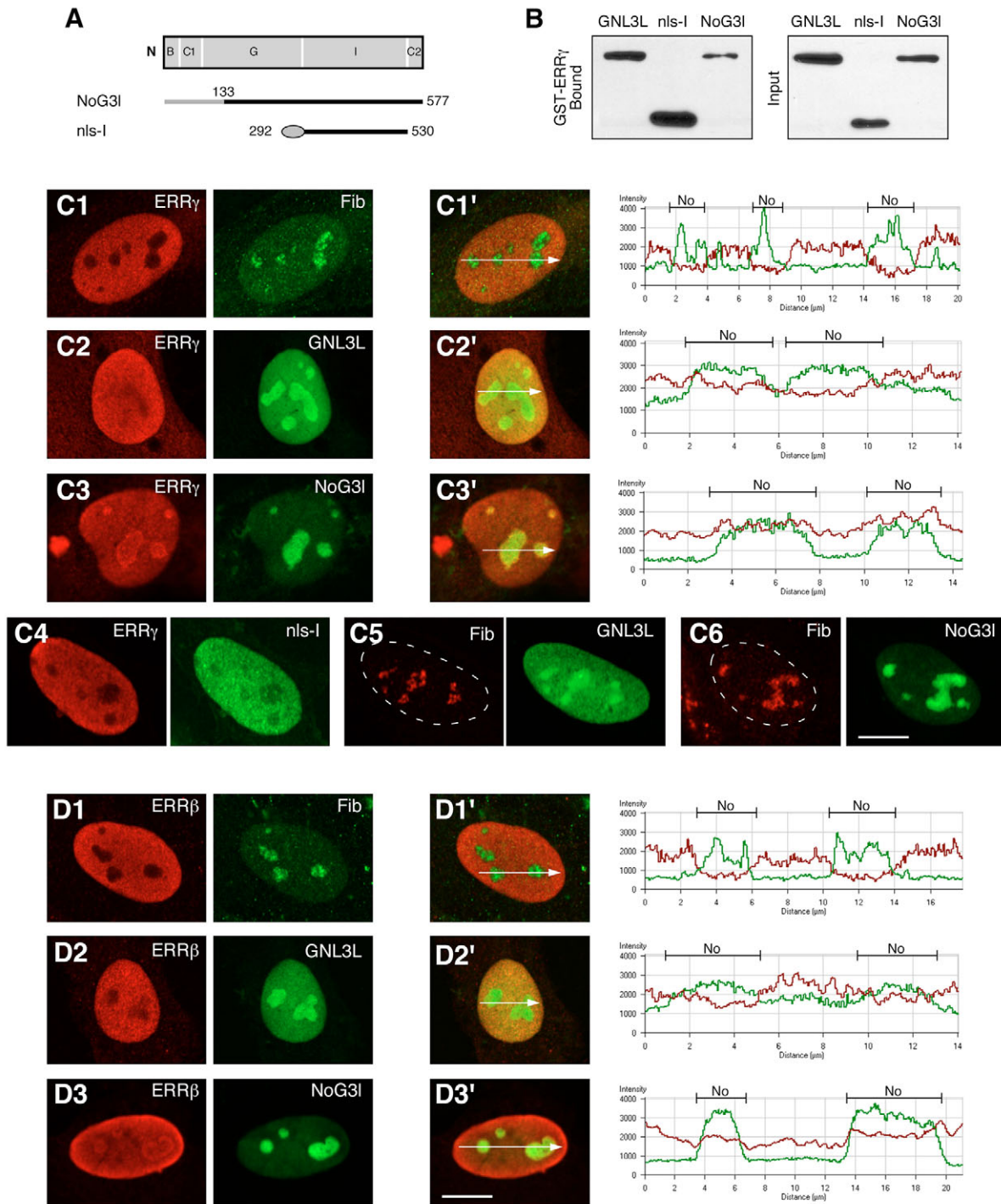


Fig. 3. Continued on next page.

fold induction seen in the siNEG-treated sample ( $25.7 \pm 1.3$  for siGNL3L-1 and  $25.3 \pm 1.0$  for siGNL3L-2;  $P < 0.0001$ ,  $n = 9$ ) (Fig. 5B). Reducing the amount of GNL3L also increased the ERR $\beta$ - and ERR $\alpha$ -mediated transactivation on the ERE-driven promoter (Fig. 5C,D). By comparison, GNL3L-specific siRNA treatment had a lesser effect on ERR $\beta$ - and ERR $\alpha$ -mediated transcription than on ERR $\gamma$ -dependent transactivation. The ERR $\alpha$  (or ERR $\beta$ )-dependent transcriptional activities were  $1.7 \pm 0.1$  (or  $6.8 \pm 0.2$ ),  $2.4 \pm 0.1$  (or  $10.7 \pm 0.3$ ), and  $2.6 \pm 0.1$  (or  $11.7 \pm 0.4$ ) in the siNEG, siGNL3L-1, and siGNL3L-2-treated samples, respectively. Together, our data demonstrate that GNL3L inhibits the transcriptional functions of the ERR genes without entering the nucleolus.

### GNL3L competes with SRC1 and SRC2 (GRIP1) for ERR $\gamma$ binding

To look for a mechanism other than nucleolar sequestration in order to explain the GNL3L-mediated inhibition of ERR transactivation, we examined the possibility that GNL3L binding of ERR $\gamma$  prevents ERR $\gamma$  from accessing coactivators, such as SRC1 and SRC2 (GRIP1), which have been shown to also bind the AF2 domain of ERR $\gamma$  (Hong et al., 1999). To test this idea, GST fusion proteins of ERR $\gamma$  were used to pull down whole-cell lysates that contained a fixed amount of SRC1 or SRC2, mixed with increasing amounts of GNL3L (Fig. 6A1,B1). In each sample, whole-cell proteins were adjusted to

the same concentration. Western blot analyses of the agarose-bound protein fractions showed that less SRC1 or SRC2 proteins were retained by GST-ERR $\gamma$  as more GNL3L protein was bound by ERR $\gamma$  [Fig. 6A1,B1, (R)]. The ability of GNL3L to compete with SRC1 and SRC2 for ERR $\gamma$  binding is abolished by a deletion of its ERR $\gamma$ -interacting I-domain (Fig. 6A2,B2). Conversely, to determine whether SRC1 or SRC2 can displace GNL3L from the ERR $\gamma$  protein complex, GST-ERR $\gamma$  fusion proteins were used to pull down a fixed amount of GNL3L in the presence of increasing amounts of SRC1 or SRC2. Our results show that both SRC1 (Fig. 6C) and SRC2 (Fig. 6D) can reduce GNL3L bound by GST-ERR $\gamma$  in a dose-dependent manner. These data demonstrate that binding between ERR $\gamma$  and GNL3L, and between ERR $\gamma$  and SRC1 or SRC2 are mutually exclusive, and suggest that blocking ERR $\gamma$  from accessing SRC1 and SRC2 may be responsible for the inhibitory transcriptional activity of GNL3L.

### Coexpression of GNL3L increases the mobility and decreases the SRC1 component of the ERR $\gamma$ DNA-protein complex

To determine whether GNL3L forms a high-order DNA-protein complex with ERR $\gamma$ , electrophoretic mobility shift assays (EMSA) were conducted using a radiolabeled probe containing a canonical ERE sequence (TCAGGTCA-CTGTGACCTGA) and cell extracts expressing the indicated

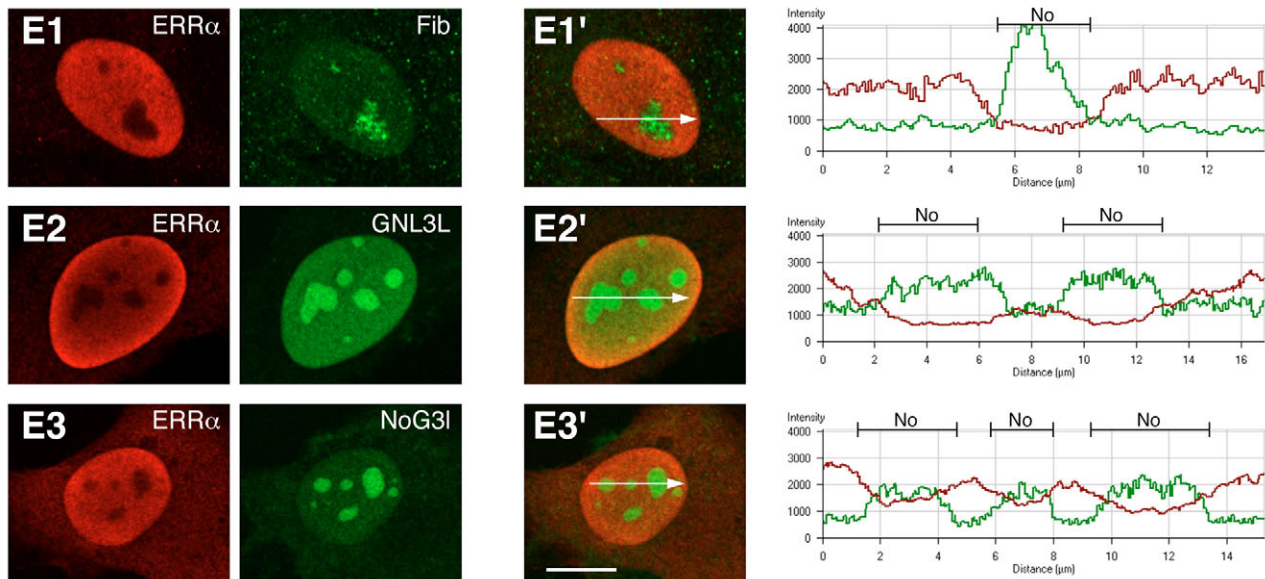


**Fig. 3.** Overexpression of GNL3L brings ERR $\beta$  and ERR $\gamma$  into the nucleolus. (A) To generate a nucleolar form of GNL3L (NoG31), we replaced the N-terminal nucleolus-targeting domain of GNL3L with the corresponding region of nucleostemin (grey bar), which has a stronger nucleolus-targeting activity than GNL3L but lacks the ability to bind ERR $\gamma$ . To create a nucleoplasmic form of GNL3L (nls-I), we fused the I-domain of GNL3L to an SV40 nuclear localization signal (oval). (B) Affinity-binding assays show that both nls-I and NoG31 maintain the ability to bind ERR $\gamma$ . To measure the effect of GNL3L overexpression on the distribution of ERR $\gamma$ , U2OS cells were transfected with Myc-tagged ERR $\gamma$  alone (C1), Myc-tagged ERR $\gamma$  and HA-tagged wild-type GNL3L (C2) or mutant GNL3L (C3,C4) or HA-tagged GNL3L constructs alone (C5 and C6). Double-transfected cells were labeled with anti-Myc (red) and anti-HA (green) antibodies, and visualized by confocal analyses. Single-transfected cells were immunostained with anti-fibrillarin antibody (Fib) and anti-Myc or anti-HA antibody. The ERR $\gamma$  (red) fluorescence intensities are measured quantitatively along the lines indicated by arrows, shown in the right panels of (C1'–C3'), and the nucleolar regions (No) are indicated by the increase of green fluorescence. Compared to cells transfected with only ERR $\gamma$ , the fluorescence intensity of ERR $\gamma$  in the nucleolus is increased in cells cotransfected with NoG31 or the wild-type GNL3L. By contrast, the nls-I mutant does not change the distribution of ERR $\gamma$  (C4). Neither does ERR $\gamma$  alter the distribution of GNL3L (C5) or NoG31 (C6). The same analyses were performed using ERR $\beta$  (D1–D3) and ERR $\alpha$  (E1–E3). Our results showed that, when coexpressed with wild-type GNL3L (D2) or NoG31 (D3), ERR $\beta$  begins to accumulate in the nucleolus. GNL3L overexpression has little or no effect on the distribution of ERR $\alpha$  (E2,E3). Bars, 10  $\mu$ m.

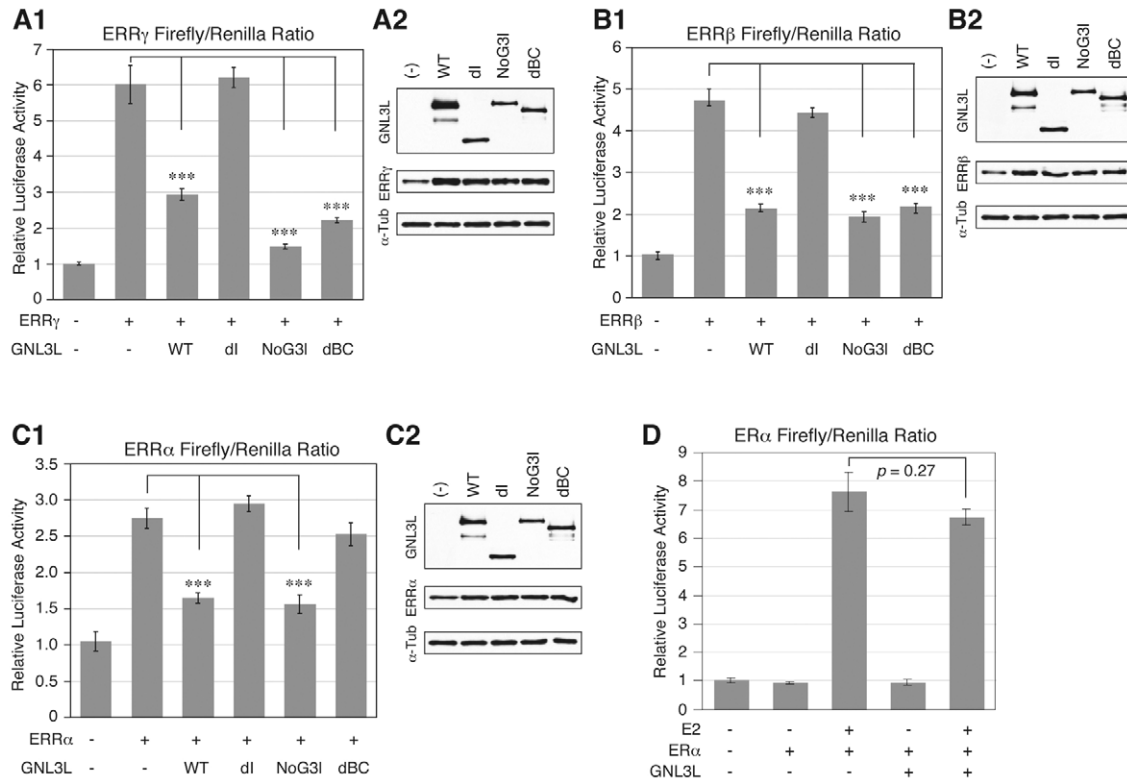


**Fig. 4.** Overexpression of GNL3L inhibits transcriptional activity of ERR proteins independently of nucleolar distribution. (A1) Estrogen response element (ERE)-specific transcriptional activities were measured in CV-1 cells by the ratio between the ERE-driven firefly luciferase activity and the *Renilla*-null luciferase activity. ERR $\gamma$  elicits a six-fold increase in the ERE-specific transcriptional activity. Coexpression of wild-type GNL3L (WT) leads to a 50% reduction in the ERR $\gamma$ -mediated transcriptional activity. This decrease is reversed by a deletion of the ERR $\gamma$ -binding I-domain of GNL3L (dI). Coexpression of either the nucleolar form (NoG3I) or the nucleoplasmic form (dBC) of GNL3L suppresses the ERR $\gamma$  transcriptional activity more than or to the same extent as the wild-type GNL3L protein. (B1,C1) Using the same approach, we show that this inhibitory activity of GNL3L can also work on (B1) ERR $\beta$  and (C1) ERR $\alpha$  with the exception that the dBC mutant has little effect on the ERR $\alpha$ -mediated transactivation. Error bars represent the standard error of the mean ( $\pm$  s.e.m.). \*\*\* $P < 0.0001$ . (A2,B2,C2) Expression levels of wild-type and mutant GNL3L proteins and ERR proteins in the experimental samples are compared in western blots side-by-side using anti-HA and anti-Myc antibodies, respectively;  $\alpha$ -tubulin ( $\alpha$ -Tub) was used as a loading control. (D) GNL3L fails to suppress the estradiol (E2)-induced transcriptional activity of ER $\alpha$  on the ERE-driven promoter in the same cell-based reporter system.

proteins (Fig. 7A). Compared with the probe alone (lane 1) and vector-transfected cell lysate samples (lane 2), the Myc-tagged ERR $\gamma$ -transfected sample (lane 3) yields an ERE-ERR $\gamma$ -specific DNA-protein complex (Fig. 7A, arrow b). The signal of this complex can be competed by excess unlabeled probes (lane 4), and supershifted by anti-Myc antibody (lane 5, arrow a). When ERR $\gamma$  was coexpressed with GNL3L, two fast-moving DNA-protein complexes were identified (arrows d and e, lane 6), and no additional slow-moving complexes were seen. The mobility of the fast-moving complexes can be retarded by anti-Myc antibody (lane 7, arrow c), but not by anti-HA antibody (lane 8), suggesting that they contain ERR $\gamma$  but not GNL3L. GNL3L alone fails to interact with the ERE probe (lane 9). The intensity of the fast-moving complex, complex d, was reduced when ERR $\gamma$  was coexpressed with a GNL3L mutant lacking its ERR $\gamma$ -binding I-domain (dI), indicating that the appearance of this fast-moving complex d depends on the interaction between GNL3L and ERR $\gamma$ .

The increased mobility of the ERR $\gamma$  DNA-protein complex by GNL3L may be caused by cleavage of the ERR $\gamma$  protein or by changes in the protein conformation or components of the ERR $\gamma$  DNA-protein complex; failure of this fast-moving

complex d to be supershifted by anti-HA antibody indicates that it does not contain GNL3L or the HA-epitope of GNL3L is masked in this particular protein conformation. To address these different possibilities, we retrieved the fast-moving and slow-moving protein complexes (complex d and complex b, respectively) from the EMSA gel and analyzed the protein amount and size of ERR $\gamma$ , GNL3L, SRC1, and SRC2 in these two complexes by western blottings (Fig. 7B). Anti-Myc western analysis shows that the size of the ERR $\gamma$  protein remains the same in both complexes, excluding the possibility that the increased mobility is a result of ERR $\gamma$  protein cleavage. Anti-HA western blotting detects no GNL3L protein in the retrieved protein complexes, consistent with the idea that GNL3L does not bind the DNA-bound ERR $\gamma$ . Notably, we are able to detect SRC1 in the slow-moving complex b but not in the fast-moving complex d, demonstrating that coexpression of GNL3L reduces SRC1 binding to the ERR $\gamma$  DNA-protein complex. Although the SRC2 protein is present in both complexes, the amount of SRC2 relative to ERR $\gamma$  is reduced in the fast-moving complex d compared with the slow-moving complex b, which suggests that SRC2 binding to ERR $\gamma$  is also diminished by GNL3L coexpression.

**GNL3L suppresses the SRC-mediated transcriptional coactivation on ERR $\gamma$**

Next, we addressed the issue whether GNL3L interferes with the function of SRC proteins as coactivators for ERR $\gamma$ . In a cell-based reporter system similar to that described in Fig. 4,

coexpression of ERR $\gamma$  and SRC1 is able to produce an eight-fold increase ( $8.0 \pm 0.3$ ) in the ERE-specific transcriptional activity compared with the control sample – which is 1.7 times higher than the sample expressing only ERR $\gamma$  ( $4.8 \pm 0.3$ ) (Fig. 8A). When coexpressed with GNL3L, the luciferase activity is

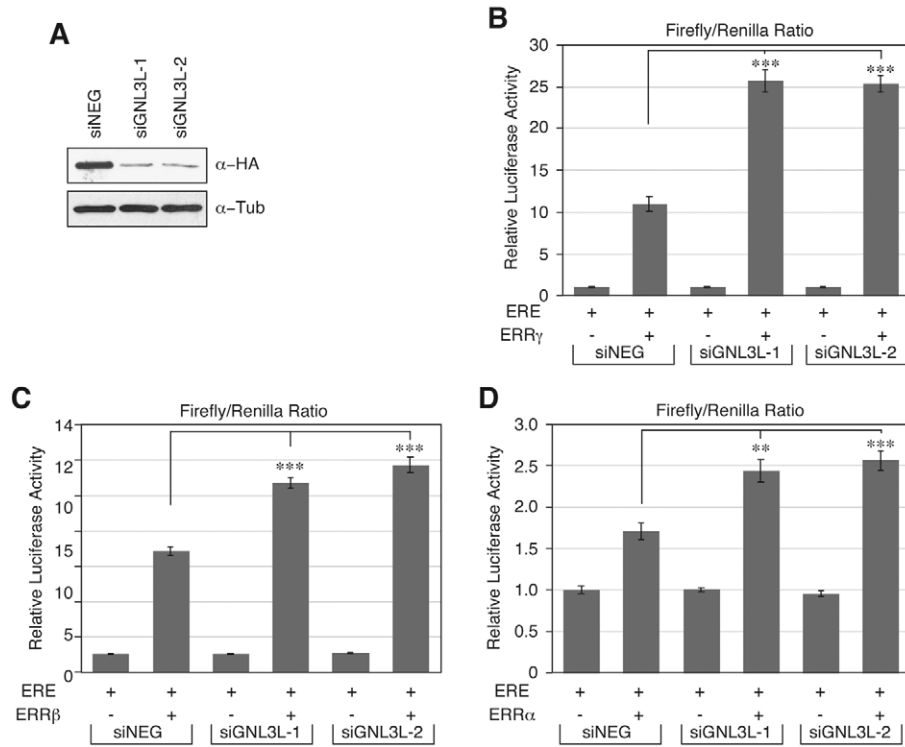


**Fig. 5.** Endogenous GNL3L suppresses transcriptional activity of ERR family genes. (A) To confirm the GNL3L-mediated negative regulation of ERR activities from a loss-of-function angle, a small interfering RNA (siRNA) approach was used to knock down the endogenous expression of GNL3L. Compared to the control knockdown sample (siNEG), the protein knockdown efficiencies of GNL3L-specific siRNA duplexes (siGNL3L-1 and siGNL3L-2) in HEK293 cells stably expressing HA-tagged GNL3L are estimated to be 83% and 84%, respectively. (B) Consistent with our overexpression data, the transcriptional activity of ERR $\gamma$  is increased 2.5 times by siGNL3L-1 and siGNL3L-2 treatment as compared with the siNEG-treated sample. (C,D) GNL3L knockdown has the same effect on the ERR $\beta$ - and ERR $\alpha$ -mediated transactivation, although their increase is less dramatic than the increase in the ERR $\gamma$ -mediated transactivation. Error bars represent the standard error of the mean ( $\pm$  s.e.m.). \*\* $P < 0.001$ ; \*\*\* $P < 0.0001$ .

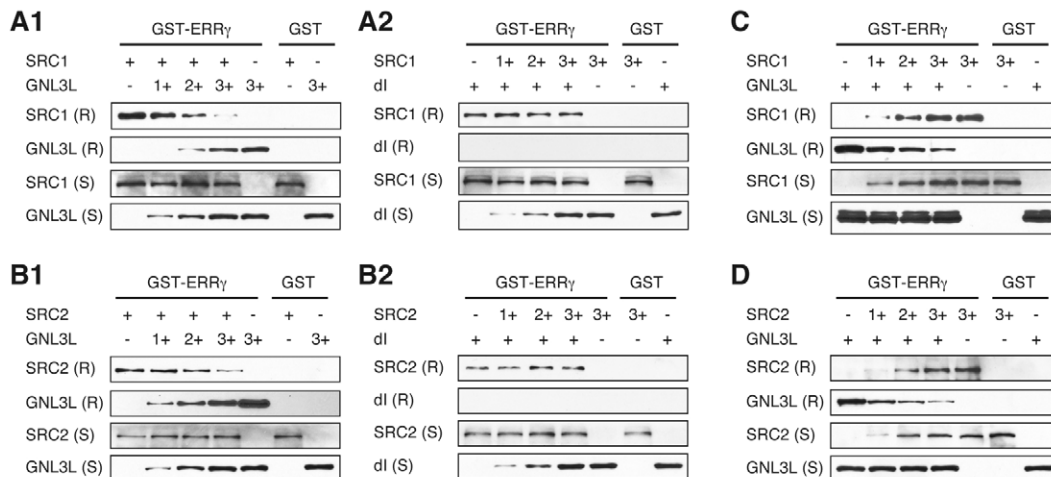


**Fig. 6.** GNL3L competes with SRC1 and SRC2 for ERR $\gamma$  binding. Agarose-bound GST fusion proteins of ERR $\gamma$  (1  $\mu$ g) were used to pull down whole-cell lysates containing a fixed amount of SRC1 (A) or SRC2 (B), mixed with increasing amounts of the wild-type GNL3L (A1,B1) or the dl mutant lacking the ERR $\gamma$ -interacting domain (A2,B2). Whole-cell proteins in each sample were adjusted to the same amount. In the agarose-retained portions (R), the interaction between GNL3L and ERR $\gamma$  can reduce the amount of SRC1 and SRC2 bound by ERR $\gamma$  in a dose-dependent manner, but the dl mutant fails to do so. Conversely, when GST-ERR $\gamma$  fusion proteins were used to pull down the same amount of GNL3L in the presence of increasing amounts of SRC1 (C) or SRC2 (D), SRC1 and SRC2 were able to reduce the amount of GNL3L bound by ERR $\gamma$  in a dose-dependent way as well. Proteins in the agarose-bound fraction and in the supernatant are indicated by (R) and (S), respectively.



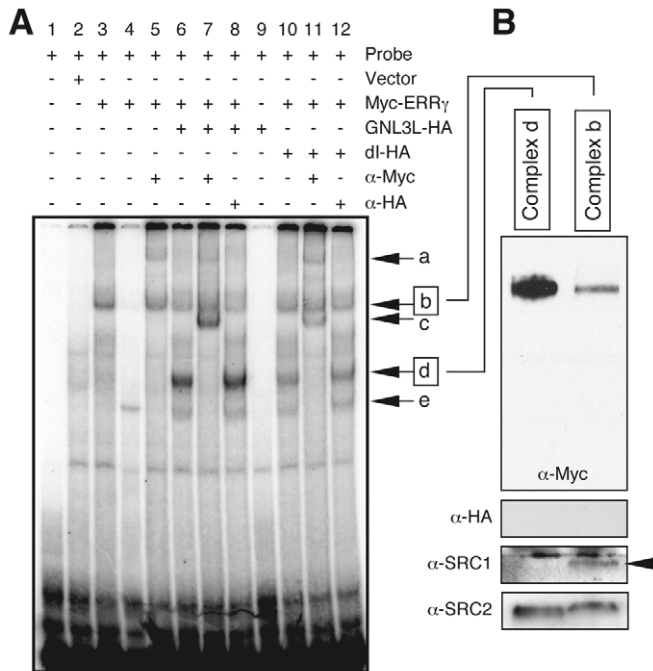


**Fig. 7.** Coexpression of GNL3L increases the electrophoretic mobility of the DNA-bound ERR $\gamma$  protein complex and reduces its binding with SRC1 and SRC2. (A) The GNL3L effect on the binding of ERR $\gamma$  to DNA was examined by EMSA using ERE-containing probes and whole-cell lysates expressing the indicated recombinant proteins. Compared with the probe alone (lane 1) and the vector-transfected control sample (lane 2), ERR $\gamma$ -specific DNA-protein complex was identified in lane 3 (arrow b), competed by excess non-labeled probes (lane 4), and supershifted by anti-Myc antibody (lane 5, arrow a). Coexpression of GNL3L produces fast-moving complexes (lane 6, arrows d and e) that can be supershifted by anti-Myc antibody (lane 7, arrow c) but not by anti-HA antibody (lane 8). GNL3L itself cannot bind the ERE probe (lane 9). The intensity of the fast-moving complex d is reduced by a deletion of the ERR $\gamma$ -binding I-domain of GNL3L (lanes 10–12). (B) The fast-moving complex d and the slow-moving complex b were retrieved from the EMSA gel, fractionated in SDS-denaturing PAGE and analyzed for their ERR $\gamma$  ( $\alpha$ -Myc), GNL3L ( $\alpha$ -HA), SRC1, and SRC2 protein components by western blotting. Our results indicate that the increase in the electrophoretic mobility of the ERR $\gamma$ -DNA complex by GNL3L coexpression is due to a loss of SRC1 binding (arrow) and diminished SRC2 binding, rather than by protein cleavage of ERR $\gamma$ .

reduced to 3.6 times ( $\pm 0.2$ , for 100 ng of GNL3L) and 2.5 times ( $\pm 0.2$ , for 200 ng of GNL3L) that of the control sample, representing respectively a 55% and 70% reduction compared with the sample expressing both ERR $\gamma$  and SRC1. Again, a deletion of the ERR $\gamma$ -interacting domain (dl) abolishes the suppressive activity of GNL3L ( $P=0.17$ ). The ability of GNL3L to inhibit the transcriptional coactivator activity can also work on SRC2 (Fig. 8B). Here, we show that GNL3L, but not the dl mutant, can reduce the ERR $\gamma$ -SRC2-mediated 7.4-fold increase ( $7.4\pm 0.2$ ) in the luciferase activity down to 3.4-fold ( $\pm 0.2$ , for 100 ng of GNL3L) and 2.1-fold ( $\pm 0.2$ , for 200 ng of GNL3L) compared with the control sample. The dl mutant fails to exhibit this inhibitory activity ( $P=0.58$ ). These data demonstrate that GNL3L can suppress the SRC1-

mediated and SRC2-mediated coactivation of ERR $\gamma$  in an I-domain-dependent manner.

## Discussion

In this manuscript, we identify a GNL3L-mediated mechanism that suppresses the transcriptional activity of ERR family genes by coactivator competition (Fig. 9). We show that ERR binding is specific to GNL3L, but not to nucleostemin or Ngp1. GNL3L and ERR $\gamma$  colocalize in the nucleoplasm, and their interaction requires the I-domain of GNL3L and the AF2-domain of ERR $\gamma$ . Gain-of-function and loss-of-function studies reveal that GNL3L has the ability to suppress the transcriptional activity of ERR genes, and does not require the nucleolar localization of GNL3L to do so. We also demonstrate that GNL3L can compete with SRC1 and SRC2 for their binding to ERR $\gamma$ , resulting in an increased electrophoretic mobility of the DNA-bound ERR $\gamma$  complex and the inhibition of the SRC1 and SRC2 coactivator function on ERR $\gamma$ . The AF2-domain binding, SRC competition and transcriptional inhibition activities suggest that GNL3L represents a new class of transcriptional co-repressor for nuclear receptors. However, GNL3L fails to form a stable complex with the DNA-bound ERR $\gamma$ , and the I-domain of GNL3L – which is necessary and sufficient for ERR $\gamma$  binding – lacks the LxxLL motif found in most transcriptional coactivators and co-repressors that interact with the AF2-domain (Hentschke et al., 2002; Huss et al., 2002; Lee et al., 1998; Rosenfeld and Glass, 2001; Webb et al., 2000; Zhang et al., 2000). These data support the role of GNL3L as a novel regulator for the ERR gene family and argue against its role as a classical transcriptional co-repressor. It is worth noting that the absence of interaction between GNL3L and the DNA-bound ERR $\gamma$  in vitro does not exclude the possibility that these two proteins still coexist in the same DNA-bound complex in the native chromatinized context, because the binding of transcription factors to the core response element in vivo is aided by a number of cofactors as well as by histone proteins involved in chromatin remodeling. Furthermore, the ability of GNL3L to compete for SRC binding and to inhibit the transcriptional function of ERR $\gamma$  might depend on specific chromatin structures or involve cofactors other than SRC proteins.

GNL3L and ERR proteins are colocalized in the nucleoplasm, but only GNL3L is also found in the nucleolus. The nucleolar localization of GNL3L might have created two potential mechanisms that affect its activity in the nucleoplasm. First, GNL3L can enter or exit the nucleolus by itself. In this case, signals that promote the nucleolar accumulation of GNL3L may cause a disinhibition of the ERR activities, and signals that release the nucleolus-bound GNL3L into the nucleoplasm may allow more GNL3L to bind ERR proteins. Alternatively, GNL3L may carry some ERR proteins with it when entering the nucleolus, in which case nucleolar sequestration of ERR proteins may account for some of the inhibitory activity of GNL3L. Although overexpression of a nucleolar form of GNL3L and, to a less extent, the wild-type GNL3L increase the nucleolar intensity of ERR $\beta$  and ERR $\gamma$ , the non-nucleolar dBC mutant is able to suppress ERR $\beta$  and ERR $\gamma$  activities as much as wild-type GNL3L. These results demonstrate that the suppressive effect of GNL3L on the ERR activity is not mediated by a nucleolar sequestration

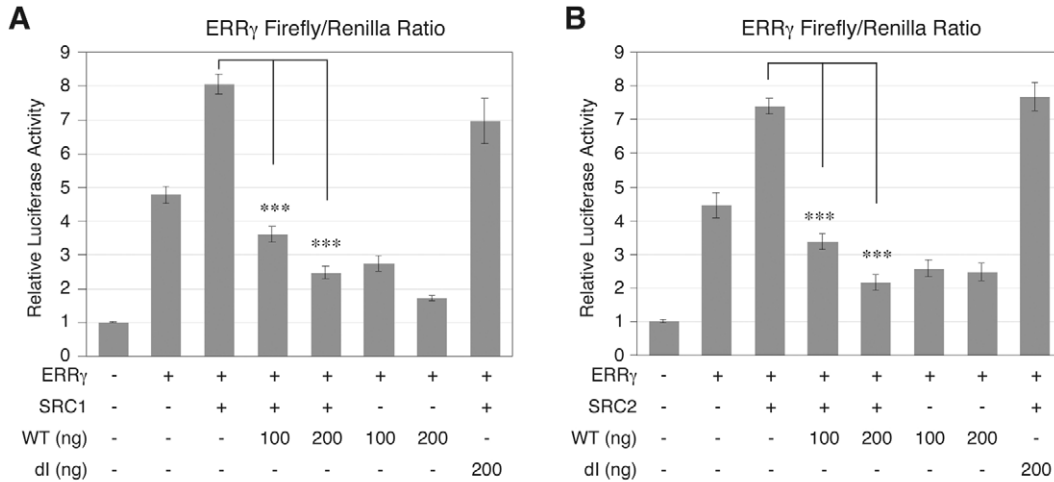


**Fig. 8.** GNL3L suppresses SRC-mediated transcriptional coactivation of ERR $\gamma$ . (A) Using the same cell-based reporter system as described in Fig. 4, we show that the ERE-specific transcriptional activity in cells coexpressing ERR $\gamma$  and SRC1 ( $8.0 \pm 0.3$ ) is 1.7 times higher than that of the ERR $\gamma$ -expressing sample ( $4.8 \pm 0.3$ ). When coexpressed with the wild-type GNL3L (WT), this ERR $\gamma$  and SRC1-mediated ERE-specific transcriptional activity is reduced by 55% and 70% compared with the sample expressing both ERR $\gamma$  and SRC1 in a dose-dependent manner. This inhibitory effect of GNL3L on the SRC1-mediated coactivation of ERR $\gamma$  requires the I-domain of GNL3L because deletion of this domain (dl) fails to suppress the transcriptional activity of ERR $\gamma$  and SRC1 ( $P=0.17$ ). (B) Using the same approach, we show that GNL3L can also suppress the coactivator function of SRC2 on the ERR $\gamma$ -dependent transcriptional activity in a dose-dependent (54% reduction for 100 ng of GNL3L and 71% reduction for 200 ng of GNL3L) and I-domain-dependent ( $P=0.58$ ) manner. Error bars represent the stand error of mean ( $\pm$  s.e.m.). \*\*\* $P < 0.0001$ .

mechanism and that, under physiological conditions, the ERR-binding and transcriptional inhibition events of GNL3L take place in the nucleoplasm. Nevertheless, the fact that overexpression of NoG3l can bring ERR $\beta$  and ERR $\gamma$  into the nucleolus supports the notion that GNL3L can interact with these two proteins in vivo.

Unlike ER $\alpha$  whose activity is controlled by hormone binding, no ligand has so far been identified for ERR family genes and their transactivation works in a ligand-independent manner. This GNL3L-mediated inhibition on the activities of ERRs provides one mechanism to regulate their functions

in a cell-context-dependent and dynamic way. At the transcriptional level, although the relative abundance of GNL3L matches that of ERR $\gamma$  in most tissues we examined, they are distinctively different in the brain and heart. GNL3L is expressed highly in the brain but little in heart, whereas ERR $\gamma$  is found at high levels in heart but not in brain. The differences between the expression levels of GNL3L and ERR $\gamma$  in those organs indicate that tissues that express the same level of ERR $\gamma$  may exhibit differential ERR activities depending on their GNL3L expression. In the adult brain where little ERR $\gamma$  is found, GNL3L might have other regulatory

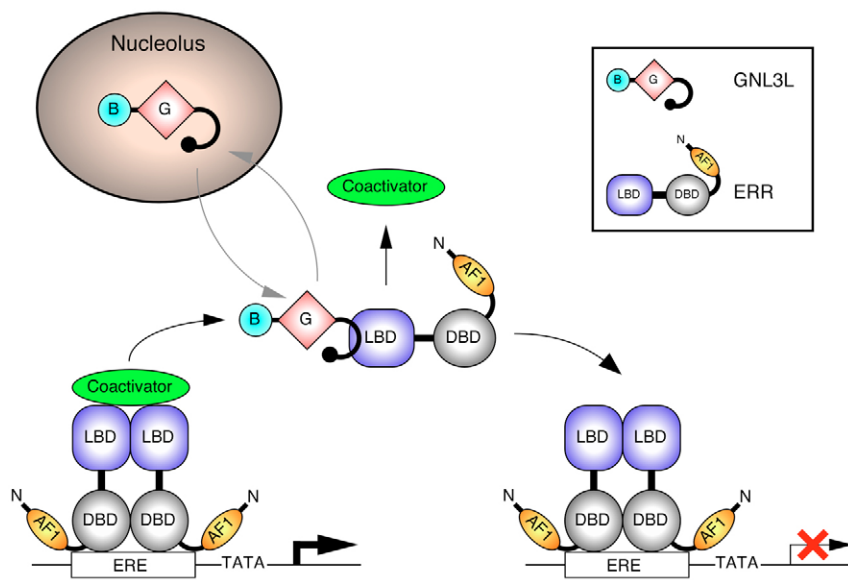


**Fig. 9.** GNL3L inhibits the transcriptional activities of ERR family genes by coactivator competition. Our data reveal a novel mechanism that regulates the activity of ERR family genes by the nucleolar GTP-binding protein GNL3L. GNL3L decreases the transcriptional activity of ERR proteins. This event takes place in the nucleoplasm and does not require the nucleolar localization of GNL3L. The interaction between GNL3L and ERR $\gamma$  displaces coactivators such as SRC1 and SRC2 from the ERR $\gamma$  complex. The SRC-depleted ERR $\gamma$  protein binds DNA without GNL3L, resulting in transcriptional inhibition. In this model, the nucleolar accumulation of GNL3L does not appear to affect its ability to suppress the transcriptional function of ERR proteins (grey arrows). Protein domains of GNL3L and ERR are: B, basic domain; C1 and C2, coiled-coil domain-1 and -2; G, GTP-binding domain; I, intermediate domain; AF1 and AF2, activation function 1 and 2; DBD, DNA-binding domain; LBD, ligand-binding domain.

targets. At the post-translational level, GNL3L is partitioned between the nucleolus and the nucleoplasm by a dynamic process (L.M. and R.Y.L.T., unpublished data). Like nucleostemin (Meng et al., 2006; Tsai and McKay, 2005), the nucleolar accumulation of GNL3L is controlled by its GTP binding and a N-terminal basic domain (Rao et al., 2006) (L.M. and R.Y.L.T., unpublished data). Notably, the nucleolar residence of GNL3L is significantly shorter than that of nucleostemin (L.M. and R.Y.L.T., unpublished data). The transient residence of GNL3L in the nucleolus might explain why nucleolar compartmentalization of GNL3L does not seem to play a role in its ability to suppress the ERR transcriptional function.

In conclusion, it is known that the ERR family genes are transcriptionally active without the ligand, but it is unclear if and how their activities can be controlled in a dynamic manner. Our work unravels a GNL3L-mediated mechanism that modulates the transcriptional activity of ERR $\gamma$  by coactivator competition. Given the important role of the ERR genes in embryogenesis and tumorigenesis, the differential regulation of their activities by GNL3L can provide us with new insight into these two processes in a cell-type-specific manner.

## Materials and Methods

### Recombinant plasmids and mutation analyses

Full-length ERR family genes were cloned from mouse brain cDNAs by reverse transcription (RT)-PCR. Deletions and point mutations of GNL3L and ERR $\gamma$  were introduced by the stitching PCR method as described previously (Tsai and McKay, 2002; Tsai and McKay, 2005). The final PCR products were subcloned into pCIS expression vectors and confirmed by sequencing.

### Cell culture, transfection, siRNA knockdown and immunostaining

We used HEK293 cells for biochemical studies because of their high transfection efficiency and protein production, and U2OS cells for distribution analyses. Cells were maintained in Dulbecco's modified Eagle's medium (DMEM) supplemented with 5% fetal bovine serum (FBS, Hyclone), penicillin (50 IU/ml), streptomycin (50  $\mu$ g/ml), and glutamine (1%). Plasmid transfections were performed using a standard Ca<sup>2+</sup> phosphate method for HEK293 cells or the Lipofectamine-Plus reagent (Invitrogen) for U2OS cells. Immunofluorescence studies were performed 1 day after transfection as described previously (Tsai and McKay, 2005). For siRNA knockdown experiments, cells were transfected with siRNA duplex (100 nM) for 12–24 hours using Oligofectamine reagent (Invitrogen) and analyzed 2 days later. Targeted sequences for siRNA duplexes were as followed: siGNL3L-1, 5'-AAA-AACGACGACCAUUGAGA-3'; siGNL3L-2, 5'-AACUAUUGCCGCCUUGG-UGAA-3'; siNEG, 5'-AAUGACGAUCAGAAUUGCGACU-3'.

Primary antibodies were monoclonal anti-HA antibody ( $\times$ 2000; HA.11, Covance), monoclonal anti-Myc antibody ( $\times$ 1000, Covance) and monoclonal anti-fibrillarin antibody ( $\times$ 1000, EnCor). Secondary antibodies were conjugated with Rhodamine-X or FITC.

### Yeast two-hybrid screen

Full-length mouse *GNL3L* was subcloned in the pAS2-1 vector and used as a bait to screen an E17.5 mouse brain cDNA library in the pACT2 vector (Clontech). The bait and library plasmids were co-transformed into the *Saccharomyces cerevisiae* strain Y190, and selected for both histidine<sup>+</sup> and  $\beta$ -galactosidase<sup>+</sup> phenotypes. cDNA plasmids were re-transformed into *Escherichia coli* HB101 by electroporation and expanded for further analysis.

### Coimmunoprecipitation

Cells were harvested in NTEN buffer (20 mM Tris pH 8.0, 150 mM NaCl, 1 mM EDTA, 0.5% NP40, 0.1 mM DTT, supplemented with 1 mM PMSF, 1  $\mu$ g/ml leupeptin, 0.5  $\mu$ g/ml aprotinin, 0.7  $\mu$ g/ml pepstatin A, and 1  $\mu$ M E64). Lysates were incubated with monoclonal anti-HA (HA.11, Covance), monoclonal anti-Myc (9E10, Covance), or mouse IgG for 1 hour, followed by incubation with protein G sepharose beads (Pharmacia) for an additional 4 hours at 4°C. Immunoprecipitates were washed 5 times with RIPA buffer (1 $\times$  PBS, 0.1% SDS, 0.5% sodium deoxycholate, 1% NP40, 1 mM PMSF, 1  $\mu$ g/ml leupeptin, 0.5  $\mu$ g/ml aprotinin, 0.7  $\mu$ g/ml pepstatin A, and 1  $\mu$ M E64), fractionated by 10% sodium dodecyl sulfate-polyacrylamide gel electrophoresis (SDS-PAGE), and transferred to Hybond-P membranes (Amersham). Specific signals were detected by western blotting with

polyclonal anti-HA or anti-Myc antibodies and horseradish-peroxidase-conjugated secondary antibody.

### Affinity binding and competition assays

Full-length cDNAs of *GNL3L* and ERR $\gamma$  were subcloned into the pGEX4T-2 vector. GST fusion proteins were expressed in BL21/DE3 as described previously (Tsai and McKay, 2002; Tsai and Reed, 1997). Epitope-tagged proteins were expressed in HEK293 cells and extracted in phosphate-buffered saline (PBS)-Triton X-100 (1% buffer, supplemented with protease inhibitors. Sepharose-bound GST fusion proteins (2–5  $\mu$ g) were incubated with whole-cell lysates for 2 hours at 4°C, washed five times with extraction buffer, including twice with high-salt buffer (extraction buffer plus 500 mM of NaCl), fractionated on 10% SDS-PAGE, and detected by western blot analyses.

### Northern blot analyses

Ten micrograms of total RNA were isolated from CD-1 mice using Trizol solutions (Invitrogen), fractionated on 1% formamide denaturing agarose gels, and transferred onto Hybond XL membrane (Amersham). Filters were then hybridized with <sup>32</sup>P-labeled probes at 65°C overnight and washed under high stringency conditions. Plaque date was counted as embryonic day 0.5 (E0.5).

### Image acquisition

Confocal images were captured on a Zeiss LSM510 confocal microscope using a 63 $\times$  plan-apochromat oil objective. Images were scanned using the multi-track program, a 512 $\times$ 512 frame size, 3 $\times$  zoom, and <1.4  $\mu$ m optical thickness. Detector gain and amplifier offset were adjusted to ensure that all signals were appropriately displayed within the linear range. Fluorescence intensities were digitally quantified in Fig. 3C',D',E' using the profile display mode along the path indicated by arrow.

### Dual luciferase assays

For gain-of-function experiments, CV1 cells were grown in DMEM supplemented with 5% charcoal/dextran-treated FBS. Transient transfection was performed in 24-well plates using the Lipofectamine-Plus reagent. Total DNA amount in each well was adjusted to 2  $\mu$ g using the empty expression vector. Cell extracts were prepared 30 hours after transfection. HEK293 cells were used for siRNA knockdown experiments because of their high GNL3L expression levels. HEK293 cells were split and grown in DMEM supplemented with 5% charcoal/dextran-treated FBS. On the next day, transfections of siRNA duplexes were performed in 24-well plates using the Oligofectamine reagent (Invitrogen). Firefly (100 ng) and *Renilla* (10 ng) reporter plasmids, ERR (50 ng), ER $\alpha$  (100 ng), GNL3L-related genes (200 ng or as specified), and/or SRC (50 ng) expression vectors were transfected on the fourth day, and cell extracts were prepared 1 day later. For E2 stimulation (Fig. 4D), cells were treated with 100 nM of E2. Firefly and *Renilla* luciferase activities were measured by the Dual-Luciferase Reporter Assay System (Promega). The expression of the firefly luciferase reporter gene was driven by three repeats of a synthetic consensus palindromic estrogen response element (ERE, GGTCACGTGACC).

### EMSA and post-EMSA western blot

Electrophoretic mobility shift assays (EMSAs) were carried out as described previously (Tsai and Reed, 1997; Tsai and Reed, 1998) with the following modifications. Recombinant proteins were expressed in HEK293 cells. Whole-cell lysates were extracted in buffer containing 40 mM HEPES-KOH (pH 7.9), 0.4 M KCl, 1 mM DTT, 10% glycerol, 0.1 mM PMSF and complete protease inhibitor cocktail (Roche) mixed with specified amounts of probes in 20  $\mu$ l binding reactions, and incubated on ice for 20 minutes. The binding-reaction mixture contained 10 mM HEPES (pH 7.9), 70 mM KCl, 2.5 mM MgCl<sub>2</sub>, 1 mM EDTA, 1 mM dithiothreitol, 4% glycerol, 20  $\mu$ g/ml salmon sperm DNA and 200  $\mu$ g/ml poly-deoxyinosinic-deoxycytidylic acid. The reaction products were subjected to electrophoresis on a 4% polyacrylamide gel (29:1) in 0.5 $\times$  Tris-borate-EDTA (TBE) buffer at 4°C, and detected by autoradiography. To generate EMSA probes, RT1006 primer was radiolabeled with [ $\gamma$ -<sup>32</sup>P]ATP in a T4 kinase reaction, annealed with excess amounts of RT1007 primer, and purified using a QIAquick nucleotide removal kit (Qiagen); RT1006, 5'-GATCTCTTTGATCAGGTCAGTGTGACCTGACTTTG-3'; RT1007: 5'-GATCCAAAGTCAGGTACAGTGACCTGATCAAAGA-3. To determine the protein components in the shifted complexes, fast (d) and slow (b) mobility complexes were identified by autoradiography, retrieved, and subjected to SDS-PAGE. Western analyses were performed using the mouse anti-Myc, rabbit anti-HA, rabbit anti-SRC1 (abcam, ab2859,  $\times$ 500), and mouse anti-SRC2 (BD Transduction Laboratories, clone 29,  $\times$ 250) antibodies.

We thank Seokwoon Kim for his technical support in the beginning of this work. SRC1 and SRC2 expression plasmids were kindly provided by Jiemin Wong, and the ERE reporter construct was kindly provided by Stephen Safe. This work was supported by a grant from the National Cancer Institute (R01 CA113750-01) to R.Y.L.T.

## References

- Ariazi, E. A. and Jordan, V. C. (2006). Estrogen-related receptors as emerging targets in cancer and metabolic disorders. *Curr. Top. Med. Chem.* **6**, 203-215.
- Baddoo, M., Hill, K., Wilkinson, R., Gaupp, D., Hughes, C., Kopen, G. C. and Phinney, D. G. (2003). Characterization of mesenchymal stem cells isolated from murine bone marrow by negative selection. *J. Cell. Biochem.* **89**, 1235-1249.
- Beekman, C., Nichane, M., De Clercq, S., Maetens, M., Floss, T., Wurst, W., Bellefroid, E. and Marine, J. C. (2006). Evolutionarily conserved role of nucleostemin: controlling proliferation of stem/progenitor cells during early vertebrate development. *Mol. Cell. Biol.* **26**, 9291-9301.
- Bonnelye, E., Vanacker, J. M., Spruyt, N., Alric, S., Fournier, B., Desbiens, X. and Laudet, V. (1997). Expression of the estrogen-related receptor 1 (ERR-1) orphan receptor during mouse development. *Mech. Dev.* **65**, 71-85.
- Bookout, A. L., Jeong, Y., Downes, M., Yu, R. T., Evans, R. M. and Mangelsdorf, D. J. (2006). Anatomical profiling of nuclear receptor expression reveals a hierarchical transcriptional network. *Cell* **126**, 789-799.
- Daigle, D. M., Rossi, L., Berghuis, A. M., Aravind, L., Koonin, E. V. and Brown, E. D. (2002). YjeQ, an essential, conserved, uncharacterized protein from *Escherichia coli*, is an unusual GTPase with circularly permuted G-motifs and marked burst kinetics. *Biochemistry* **41**, 11109-11117.
- Du, X., Rao, M. R., Chen, X. Q., Wu, W., Mahalingam, S. and Balasundaram, D. (2006). The homologous putative GTPases Grn1p from fission yeast and the human GNL3L are required for growth and play a role in processing of nucleolar pre-rRNA. *Mol. Biol. Cell* **17**, 460-474.
- Giguere, V., Yang, N., Segui, P. and Evans, R. M. (1988). Identification of a new class of steroid hormone receptors. *Nature* **331**, 91-94.
- Hentschke, M., Susens, U. and Borgmeyer, U. (2002). PGC-1 and PERC, coactivators of the estrogen receptor-related receptor gamma. *Biochem. Biophys. Res. Commun.* **299**, 872-879.
- Hong, H., Yang, L. and Stallcup, M. R. (1999). Hormone-independent transcriptional activation and coactivator binding by novel orphan nuclear receptor ERR3. *J. Biol. Chem.* **274**, 22618-22626.
- Huss, J. M., Kopp, R. P. and Kelly, D. P. (2002). Peroxisome proliferator-activated receptor coactivator-1alpha (PGC-1alpha) coactivates the cardiac-enriched nuclear receptors estrogen-related receptor-alpha and -gamma. Identification of novel leucine-rich interaction motif within PGC-1alpha. *J. Biol. Chem.* **277**, 40265-40274.
- Kaffenah, W., Mistry, S., Williams, C. and Hollander, A. P. (2006). Nucleostemin is a marker of proliferating stromal stem cells in adult human bone marrow. *Stem Cells* **24**, 1113-1120.
- Kallen, J., Schlaeppli, J. M., Bitsch, F., Filipuzzi, I., Schilb, A., Riou, V., Graham, A., Strauss, A., Geiser, M. and Fournier, B. (2004). Evidence for ligand-independent transcriptional activation of the human estrogen-related receptor alpha (ERRalpha): crystal structure of ERRalpha ligand binding domain in complex with peroxisome proliferator-activated receptor coactivator-1alpha. *J. Biol. Chem.* **279**, 49330-49337.
- Kallstrom, G., Hedges, J. and Johnson, A. (2003). The putative GTPases Nog1p and Lsg1p are required for 60S ribosomal subunit biogenesis and are localized to the nucleus and cytoplasm, respectively. *Mol. Cell. Biol.* **23**, 4344-4355.
- Lee, C. H., Chinpaisal, C. and Wei, L. N. (1998). Cloning and characterization of mouse RIP140, a corepressor for nuclear orphan receptor TR2. *Mol. Cell. Biol.* **18**, 6745-6755.
- Leipe, D. D., Wolf, Y. I., Koonin, E. V. and Aravind, L. (2002). Classification and evolution of P-loop GTPases and related ATPases. *J. Mol. Biol.* **317**, 41-72.
- Luo, J., Sladek, R., Bader, J. A., Matthysen, A., Rossant, J. and Giguere, V. (1997). Placental abnormalities in mouse embryos lacking the orphan nuclear receptor ERR-beta. *Nature* **388**, 778-782.
- Luo, J., Sladek, R., Carrier, J., Bader, J. A., Richard, D. and Giguere, V. (2003). Reduced fat mass in mice lacking orphan nuclear receptor estrogen-related receptor alpha. *Mol. Cell. Biol.* **23**, 7947-7956.
- Meng, L., Yasumoto, H. and Tsai, R. Y. (2006). Multiple controls regulate nucleostemin partitioning between nucleolus and nucleoplasm. *J. Cell Sci.* **119**, 5124-5136.
- Rao, M. R., Kumari, G., Balasundaram, D., Sankaranarayanan, R. and Mahalingam, S. (2006). A novel lysine-rich domain and GTP binding motifs regulate the nucleolar retention of human guanine nucleotide binding protein, GNL3L. *J. Mol. Biol.* **364**, 637-654.
- Rosenfeld, M. G. and Glass, C. K. (2001). Coregulator codes of transcriptional regulation by nuclear receptors. *J. Biol. Chem.* **276**, 36865-36868.
- Sun, P., Sehoul, J., Denkert, C., Mustea, A., Konsgen, D., Koch, I., Wei, L. and Lichtenegger, W. (2005). Expression of estrogen receptor-related receptors, a subfamily of orphan nuclear receptors, as new tumor biomarkers in ovarian cancer cells. *J. Mol. Med.* **83**, 457-467.
- Suzuki, T., Miki, Y., Moriya, T., Shimada, N., Ishida, T., Hirakawa, H., Ohuchi, N. and Sasano, H. (2004). Estrogen-related receptor alpha in human breast carcinoma as a potent prognostic factor. *Cancer Res.* **64**, 4670-4676.
- Tsai, R. Y. and Reed, R. R. (1997). Cloning and functional characterization of Roaz, a zinc finger protein that interacts with O/E-1 to regulate gene expression: implications for olfactory neuronal development. *J. Neurosci.* **17**, 4159-4169.
- Tsai, R. Y. and Reed, R. R. (1998). Identification of DNA recognition sequences and protein interaction domains of the multiple-Zn-finger protein Roaz. *Mol. Cell. Biol.* **18**, 6447-6456.
- Tsai, R. Y. and McKay, R. D. (2002). A nucleolar mechanism controlling cell proliferation in stem cells and cancer cells. *Genes Dev.* **16**, 2991-3003.
- Tsai, R. Y. and McKay, R. D. (2005). A multistep, GTP-driven mechanism controlling the dynamic cycling of nucleostemin. *J. Cell Biol.* **168**, 179-184.
- Webb, P., Anderson, C. M., Valentine, C., Nguyen, P., Marimuthu, A., West, B. L., Baxter, J. D. and Kushner, P. J. (2000). The nuclear receptor corepressor (N-CoR) contains three isoleucine motifs (I/LXXII) that serve as receptor interaction domains (IDs). *Mol. Endocrinol.* **14**, 1976-1985.
- Zhang, H., Thomsen, J. S., Johansson, L., Gustafsson, J. A. and Treuter, E. (2000). DAX-1 functions as an LXXLL-containing corepressor for activated estrogen receptors. *J. Biol. Chem.* **275**, 39855-39859.
- Zhu, Q., Yasumoto, H. and Tsai, R. Y. (2006). Nucleostemin delays cellular senescence and negatively regulates TRF1 protein stability. *Mol. Cell. Biol.* **26**, 9279-9290.